ACS OMEGA

Open Access

http://pubs.acs.org/journal/acsodf

Article

Enhanced Antioxidation and UV-Absorption Ability of Industrial Lignin via Promoting Phenolic Contents and Hydrophilicity

Lili He, Haiping Guo, Jiayue Lu, Qiyu Liu,* and Xueqing Qiu*

Cite This: *ACS Omega* 2025, 10, 6745−6752

Read Online

ACCESS | Metrics & More | Article Recommendations | Supporting Information

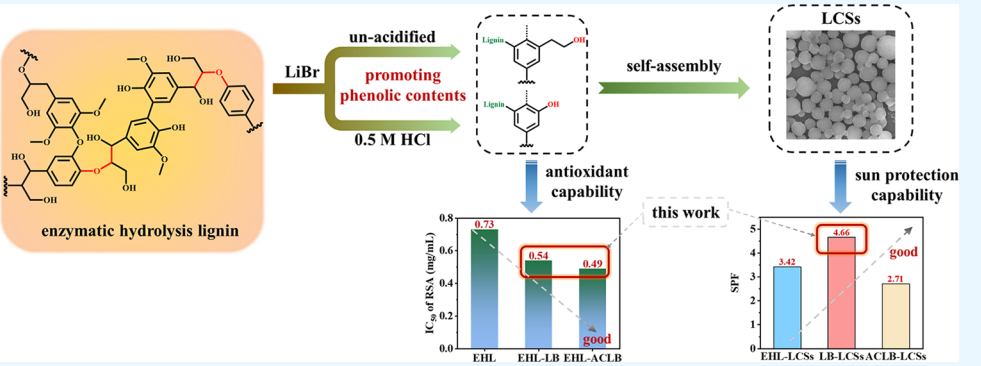

ABSTRACT: Lignin possesses unique natural antioxidation and UV-absorption abilities, making it a promising ingredient for sunscreen. However, the industrial lignin produced from pulping or bioethanol production generally shows low efficiency due to the limited phenolic hydroxyl content and poor compatibility with sunscreen, respectively. To address this issue, a molten salt hydrate treatment process was carried out for the selective cleavage of ether bonds in industrial lignin. After treatment, a 2-fold increase in phenolic hydroxyl content was observed, and lignin antioxidation efficiency was improved. The intermolecular forces of lignin in water measured by an atomic force microscope showed a significant decrease from −1.46 to 0.46 mN/m, suggesting an efficient increase in lignin hydrophilicity, which promoted lignin compatibility with sunscreen. We converted industrial lignin into colloidal balls, which improved compatibility and dispersion in the cream and more than tripled the sun protection factor compared to the direct addition of industrial lignin.

1. INTRODUCTION

The free radical oxidation and ultraviolet (UV) radiation are two critical threats to human skin health which can cause erythema, aging, and cancers.[1,2] Natural substances for antioxidation and anti-UV radiation have been studied for centuries due to their high biocompatibility and safety for the human body.[3] Lignin, the most abundant aromatic polymer existing in lignocellulose, is unique in antioxidation and UV light absorption.[4,5] Namely, the phenolic hydroxyl (−OH) groups are efficient in radical scavenging[6,7] while the massive lignin functional groups such as ketone, quinone, and chromophores are effective in UV absorption,[8−12] offering a potential application of lignin as an active ingredient in sunscreens.[9,13,14]

However, the industrial lignin derived from the pulping or bioethanol industry generally shows low efficiency in antioxidation and UV absorption, resulting from limited phenolic hydroxyl group contents and poor hydrophilicity in sunscreen dispersion.[9] To address these issues, various methods have been developed. In order to improve phenolic hydroxyl groups, homogeneous acid treatment (e.g., H_2SO_4, HCl, and H_3PO_4),[15−17] heterogeneous acid treatment (e.g., phosphotungstic, phosphomolybdic, and silicotungstic acids),[18] or alkali[19] treatment has been employed to remove impurities such as sugars[15] as well as facilitate ether bond cleavage, resulting in an increase in phenolic hydroxyl groups and therefore promoting radical scavenging rate and activity.[18] Although acid or alkali pretreatments effectively improve phenolic hydroxyl group contents, a possible reaction between electropositive Cα sites and electronegative benzene rings generally occurs under harsh conditions, leading to lignin structural condensation and aggregation,[20] further decreasing its hydrophilicity and therefore reducing its dispersity in sunscreens and leading to efficiency decline.[21,22] In order to improve lignin hydrophilicity, some modification methods have been adopted. Sulfonation modification can effectively

Received: September 19, 2024
Revised: January 17, 2025
Accepted: January 23, 2025
Published: February 13, 2025

https://doi.org/10.1021/acsomega.4c08618
ACS Omega 2025, 10, 6745−6752

improve lignin hydrophilicity via introducing sulfonate groups, but it may have potential hazards such as skin allergy.[23] Selective demethylation modification using chemical[24] or microbial[25] methods can enhance lignin hydrophilicity by increasing hydroxyl group contents, but the processes are generally complex and time-consuming. Grafting reaction shows high efficiency in increasing lignin hydrophilicity via introducing hydrophilic groups, and some functional groups such as 3,4-dihydrocoumarin (DHC) and epoxide (EPO) can also improve UV-absorbing efficiency which benefits sunscreens.[26] However, the cost and safety of grafted functional groups need further evaluation for industrial applications. Additionally, adjusting the lignin aggregation state via transforming molecules into lignin colloidal spheres (LCSs), with most of the active hydroxyl groups exposed on the particle surfaces, can improve the lignin activity and dispersity in sunscreens.[27−29] Compared with conventional modification methods, this self-assembly method provides a sustainable and efficient way to increase the available hydroxyl groups without massive chemical utilization and uncertain chemical group introduction, which is commercial and safe.

Recently, it has been reported that the molten salt hydrate (MSH), a specific concentrated inorganic salt solution, with a water-to-salt mole ratio higher than the coordinate number of cations, is unique in lignin ether bond cleavage without causing serious structural condensation and aggregation.[30,31] Therefore, MSH treatment can theoretically improve lignin antioxidation performance via promoting phenolic hydroxyl group contents as well as ensuring high hydrophilicity via inhibiting lignin condensation. In this work, industrial lignin was pretreated with unacidified and acidified MSH for selective depolymerization, followed by self-assembly to form LCSs. The structural characteristics, antioxidation, and sunscreen performance of samples were analyzed to investigate the effects of MSH treatment on lignin. After the stepwise modification, an approximately two times increase in phenolic hydroxyl groups was observed, which significantly increased the antioxidation ability. The LCSs prepared from modified lignin showed high hydrophilicity and dispersibility in sunscreens, resulting in more than twice the sun protection factor (SPF) value increase. This study offers an easy-to-operate and efficient way to improve the valorization of industrial lignin in antioxidation and UV absorption.

2. MATERIALS AND METHODS

2.1. Materials. Enzymatic hydrolysis lignin (EHL) was provided by Shandong Longlive Biotechnology Co., Ltd. Potassium bromide (KBr, 99.0%) and lithium bromide (LiBr, 99%) were purchased from Aladdin Co. Ltd., China. Hydrochloric acid (HCl, 36.0−38.0%) and acetone (99.7%) were procured from Guangzhou Anjiehui Trading Co. Ltd. 1,4-Dioxane (≥99.0%), methanol (≥99.0%), acetyl chloride, deuterated dimethyl sulfoxide (DMSO-d6, 99.9%), and pyridine-d5 (99.5%) were purchased from Guangzhou Wego Technology Co. Ltd. 2,2-Diphenyl-1-picrylhydrazyl (DPPH, 98.0%) was purchased from Guangzhou Kuanlin Instrument Technology Co. Ltd. Acetic acid (CH_3COOH, 99.7%) was provided by Guangzhou Baijun Technology Co. Ltd. Polydimethyl diallyl ammonium chloride (PDAC) was purchased from Tianjin Xiensi Biochemical Technology Co., Ltd. Deuterated chloroform ($CDCl_3$, 99.8%), tetrahydrofuran (THF, 99.0%), and 2-chloro-4,4,5,5-tetramethyl-1,3,2-dioxaphospholane (TMDP, 95.0%) were purchased from Guangzhou Rongman Biotechnology Co. Ltd. Chromium(III) acetylacetonate (98.0%) was purchased by Shanghai McLean Biochemical Technology Co. Ltd. Cyclohexanol (>99.0%) was purchased from Guangzhou Mulan Biochemical Technology Co. Ltd. The pure cream (NIVEA pure cream) was bought from Jingdong Mall; the production license number was Shanghai Makeup 20160022. All chemicals were used directly without further purification. SiO_2 standard particles (diameter of 19.9 μm) were purchased from Suzhou Nanomicro Technology Co., Ltd. (Jiangsu, China). SiO_2 substrates (1.0 × 1.0 cm) were purchased from Guangzhou Lige Technology Co., Ltd. (Guangzhou, China). NP-O10 tipless atomic force microscopy (AFM) cantilevers were purchased from Bruker (Germany).

2.2. Lignin Treatment with MSH of LiBr. EHL was dried in an oven at 60 °C for 24 h to remove adsorbed water prior to use. The MSH of LiBr was prepared by dissolving 12 g of LiBr in 8 g of deionized water, and the acid concentration in the lithium bromide solution was adjusted with hydrochloric acid. Subsequently, 2 g of EHL was added to a 15 mL thick-wall glass reactor containing 20 g of MSH, and the mixture was then transferred into an oil bath preheated to 110 °C with magnetic stirring at a speed of 200 rpm for a duration of 2 h. Following the reaction, the mixture was cooled to −20 °C and washed with deionized water to eliminate salts. The modified lignin was collected via filtration and subsequently dried in an oven at 60 °C for another period lasting up to 24 h. The modified lignin samples were denoted as EHL-LB (enzymatic lignin treated with unacidified MSH of LiBr) and EHL-ACLB (enzymatic lignin treated with acidified MSH of LiBr with an HCl concentration of 0.5 mol/L).

2.3. LCS Preparation. The lignin-based colloidal spheres (LCSs) were synthesized from different lignin samples, including native EHL, EHL treated with unacidified MSH of LiBr (EHL-LB), and EHL treated with acidified MSH of LiBr (EHL-ACLB), using an antisolvent self-assembly method. The lignin sample was initially dissolved in a mixture of acetone and water at varying concentrations (2, 4, and 6 mg/mL). Subsequently, deionized water was slowly added dropwise to the lignin solvent at a constant rate of 2.5 mL/min with magnetic stirring at 450 rpm. Following self-assembly, the LCSs were collected by centrifugation at 10,000 rpm for 10 min and washed with deionized water. After vacuum freeze-drying for 24 h to remove residual water, the resulting LCSs were named as EHL-LCSs, LB-LCSs, and ACLB-LCSs based on their respective precursor materials—EHL, EHL-LB, and EHL-ACLB.

2.4. Lignin and LCS Structure Characterization. The molecular weight of lignin samples was determined using the Agilent 1260 Infinity II gel permeation chromatography (GPC) system (Agilent, US). THF served as the mobile phase at a flow rate of 1 mL/min. In brief, 2 mg of acetylated lignin sample was dissolved in 1 mL of THF and subsequently purified using a 0.45 μm syringe filter prior to analysis.

The lignin samples were analyzed for functional groups using Fourier transform infrared spectroscopy (FT-IR, Thermo Fisher-iS50R, US) with KBr powder as the background.

The contents of phenolic hydroxyl and alcohol hydroxyl groups in lignin were calculated using ^{31}P NMR spectra. Briefly, 30 mg of sample was dissolved in 0.5 mL of a mixture of pyridine-d5 and $CDCl_3$ with a volume ratio at 1.6:1. Then, 100 μL of cyclohexanol with a concentration of 18.0 mg/mL in pyridine-d5/$CDCl_3$ was used as an internal standard, and 100

https://doi.org/10.1021/acsomega.4c08618
ACS Omega 2025, 10, 6745−6752

μL of the relaxation reagent of chromium acetylacetonate with a concentration of 5.0 mg/mL in pyridine-d5/$CDCl_3$ was added into the solution. 100 μL of the phosphorylating reagent TMDP was then added before analysis. The ^{31}P NMR of lignin samples was then tested on an Avance III HD 600 MHz spectrometer (Bruker, Switzerland) at room temperature.

The chemical linkages inside lignin were quantified by nuclear magnetic resonance (NMR) spectra. Namely, 0.5 g of lignin sample was added into a round-bottomed flask with 10 mL of acetylation reagent consisting of acetyl chloride and glacial acetic acid with a volume ratio at 1:4. After treatment at 2 h for 40 °C, the solvent was removed by evaporation at 40 °C using a rotary evaporator. The solid part was washed with deionized water and vacuum freeze-dried for 24 h. 40 mg of acetylated lignin was dissolved in 0.5 mL of DMSO-d6. The ^{1}H NMR and 2D HSQC NMR spectra of acetylated lignin were determined on an Avance III HD 600 MHz spectrometer (Bruker, Switzerland) at room temperature.

Due to the susceptibility of LCSs to deconstruction in alkaline solutions, the UV adsorption performance of LCSs was assessed using a solid sample holder UV-1900i (Shimadzu Co., Japan). The baseline was established with pure $BaSO_4$ as the background, and the test wavelength ranged from 290 to 400 nm. Prior to detection, 10 mg of lignin nanospheres were thoroughly ground and mixed with 2 g of $BaSO_4$.

The morphologies of the lignin and LCSs were observed by using scanning electron microscopy (SEM, SU8220, Hitachi, Japan). Samples were prepared by sticking lignin powder onto conductive tape and dropping a diluted lignin nanosphere solution onto silica slides, followed by drying at room temperature. The average particle sizes of LCSs were determined using a laser diffraction particle size analyzer (Mastersizer 3000, UK). Morphological characteristics of lignin sunscreen samples were observed by using an optical electron microscope (M3LY630T, Bo Shunyu Instrument Co., Ltd.).

2.5. Antioxidation Performance Determination. The antioxidation efficiency of lignin was evaluated by determining its ability to scavenge DPPH radicals as described in previous work.[32] Specifically, lignin samples were dissolved in 0.1 mL of 1,4-dioxane/water (9:1, v:v) in different concentrations (0.4−2.0 mg/mL). Then, 3.9 mL of DPPH methanol solution (1×10^{-4} mol/L) was added. The absorbance of the mixture was recorded after 60 min at 517 nm by the spectrophotometer. The equation for calculating the ratio of scavenging DPPH (RSA) was

$$\mathrm{RSA}(\%) = \frac{A_0 - A_S}{A_0} \times 100\%$$

where A_0 is the absorbance of the DPPH methanol solution at 517 nm and A_S is the absorbance of the lignin and DPPH methanol solution mixture at 517 nm, respectively. The IC_{50} value refers to the concentration of antioxidant chemicals required to achieve 50% inhibition of DPPH radicals. The lower IC_{50} value of the tested sample reflects stronger antioxidant capability.

2.6. Lignin-Doped Sunscreen Preparation. The lignin-doped sunscreens were prepared according to the method described before.[33] All lignin-doped sunscreens were prepared by blending lignin samples with pure creams without additional sunscreen actives being used. For example, 2 wt % of lignin-doped sunscreen was prepared by blending 0.02 g of lignin samples and 0.98 g of pure creams at 500 rpm for 24 h at room temperature in the dark. The lignin samples were applied at 2 mg/cm^2 to the 3M Transpore tape (7.5 cm^2) that was attached to the surface of a quartz plate. They were then spread over the tape by slowly rubbing the slide surface with a thimble-coated finger. Then, the prepared samples were dried in a dark room to block light for 30 min. The UV transmittance was measured using a solid sample holder UV-1900i (Shimadzu Co., Japan). UV transmittance data were scanned in the range of 290−400 nm. After measuring the UV transmittance, an in vitro evaluation of the SPF was conducted using the following equation:

$$\mathrm{SPF} = \frac{\Sigma_{290}^{400} E_\lambda S_\lambda}{\Sigma_{290}^{400} E_\lambda S_\lambda T_\lambda}$$

where E_λ is erythemal spectral effectiveness, S_λ is solar spectral effectiveness, W m^{-1} nm^{-1}, and T_λ is the spectral transmittance of the sample.

2.7. Lignin-Coated AFM Colloid Probe and Substrate Preparation. The molecular interaction forces among lignin were determined by AFM via a force spectroscopy module in water to provide a quantitative evaluation of lignin hydrophilicity.[34,35] The highest adhesive force values between the lignin-coated probe and the substrate were detected 75 times. The lignin with low intermolecular adhesive force in water exhibits high hydrophilicity. The lignin-coated SiO_2 particles were prepared according to the previous work with minor modifications.[35] Briefly, a drop of SiO_2 particle dispersion with a diameter of 19.9 μm was mixed with 10 mL of piranha solution for 1 h to introduce Si−O$^-$ negative charges. Subsequently, the treated SiO_2 particles were immersed in a 0.02 mM PDAC solution for 1 h to introduce positive charges. Then, the particles were placed into 1 g/L EHL alkaline solutions (pH 11.0) to adsorb lignin molecules which have negative charges. Finally, a hot-melt adhesive was applied to stick an EHL-coated SiO_2 particle to a tipless AFM cantilever with assistance from an optical microscope component. The lignin-coated substrate of 1.0 × 1.0 cm SiO_2 was prepared using the same method.

3. RESULTS AND DISCUSSION

3.1. Characteristics of MSH Treated Lignin. The characteristics of EHL, unacidified EHL-LB, and 0.5 M HCl acidified EHL-ACLB were analyzed to investigate the impact of MSH treatment on lignin structure modifications. The molecular weight of lignin decreased from 6292 to 5480 g/mol after pretreatment with unacidified MSH (Table 1), attributed to the cleavage of lignin ether bonds[30] and a potential increase in hydroxyl groups. Interestingly, it was observed that following treatment with acidified MSH, the modified EHL-ACLB exhibited a higher molecular weight of 5901 g/mol compared to EHL-LB. These results indicate that while increased acidity

Table 1. Molecular Weight of EHL, EHL-LB, and EHL-ACLB

	molecular weight		
samples	M_w (g/mol)	M_n (g/mol)	PDI
EHL	6292	4142	1.519
EHL-LB	5480	3841	1.426
EHL-ACLB	5901	4065	1.451

https://doi.org/10.1021/acsomega.4c08618
ACS Omega 2025, 10, 6745−6752

can promote ether bond cleavage, structural condensation simultaneously occurs, leading to an increase in molecular weight. Therefore, both the efficiency of ether bond cleavage and the degree of structural condensation need to be considered for enhancing sunscreen efficacy. Additionally, PDI results listed in Table 1 also revealed a decrease in heterogeneity post-MSH treatment, which is beneficial for tailored product development for specific applications.

The functional groups of lignin samples were analyzed using FT-IR to investigate the impact of MSH treatment on changes in lignin structure (Figure 1).[36] It was observed that the peak

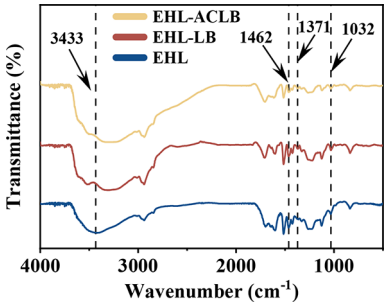

Figure 1. FT-IR spectra of EHL, EHL-LB, and EHL-ACLB.

at 3433 cm^{-1} corresponding to the stretching vibration of hydroxyl groups strengthened and shifted to a lower wavenumber after MSH treatment, indicating a significant increase in hydroxyl groups.[37] After MSH treatment, the peaks at 1462 cm^{-1} referring to methoxy groups weakened, demonstrating hydrolysis of the methoxy group to form hydroxyl groups. The peaks of EHL-LB and EHL-ACLB at 1371 cm^{-1} (in-plane bending vibration of O−H) became stronger compared with those of EHL, implying the formation of new phenolic OH groups. Similarly, low peaks at 1032 cm^{-1} related to the symmetric stretching vibration of C−O−C of ether bonds were observed in EHL-LB and EHL-ACLB, which proved the catalytic cleavage of ether bonds in MSH.

The hydroxyl groups including phenolic and aliphatic hydroxyl groups in EHL, EHL-LB, and EHL-ACLB were quantified by ^{31}P NMR with spectra shown in Figure 2 and hydroxyl group contents listed in Table 2. After MSH treatment with or without acid, the phenolic hydroxyl group peaks corresponding to syringyl −OH, guaiacy −OH, and *p*-hydroxy −OH at 142.0−143.3, 138.6−139.9, and 137.1−138.1 ppm[38] significantly decreased (Figure 2), respectively, resulting in an increase in total phenolic groups from 1.380 mmol/g of

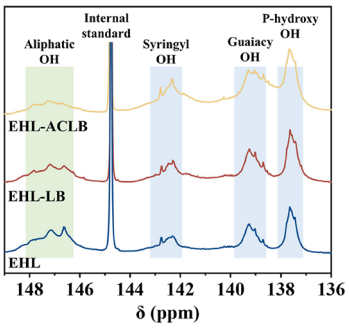

Figure 2. Quantitative ^{31}P NMR spectrum of EHL, EHL-LB, and EHL-ACLB derivatized with TMDP using cyclohexanol as the internal standard.

Table 2. Phenolic, Aliphatic, and Carboxylic Hydroxyl Contents of Different Lignin Samples Determined by ^{31}P NMR

	hydroxyl (mmol/g)				
	phenolic				
samples	H	G	S	total phenolic	aliphatic
EHL	0.392	0.414	0.574	1.380	1.187
EHL-LB	0.916	0.890	0.786	2.592	1.065
EHL-ACLB	1.114	1.551	1.241	3.906	0.774

EHL to 2.592 mmol/g of EHL-LB and 3.906 mmol/g of EHL-ACLB (Table 2). Besides, a slight decrease in aliphatic groups was also observed, possibly due to the condensation reactions.[20]

To further investigate changes in lignin structure following MSH treatment, the samples were analyzed using 2D HSQC NMR to examine specific linkages.[31,39] As depicted in Figure 3, the typical *β*-O-4 peak at $\delta C/\delta H$ = 61.28/3.55 ppm was observed in all samples. The EHL exhibited a limited content of 9.33%, attributed to the cleavage of chemical linkages during industrial bioethanol production processes. Subsequent un-acidified and acidified MSH treatments resulted in further cleavage of the *β*-O-4 linkage to 7.54 and 7.37%, respectively (Figure 3). Additionally, analysis of the ^{1}H NMR results presented in the Supporting Information revealed a clear decrease in methoxy group content (Figure S1). The cleavage of these ether bonds led to an increase in the hydroxyl group content, consistent with the findings from the ^{31}P NMR analysis.

3.2. Antioxidation Performance of MSH Pretreated Lignin. The structure analysis results showed an effective increase in phenolic hydroxyl groups after MSH treatment, which has a positive effect on antioxidation. In order to quantify radical scavenging ability (RSA) of different lignin samples,[40,41] the degradation of DPPH radicals was carried out in the presence of dissolved lignin. After being neutralized by lignin, the DPPH radicals were transformed into hydrazine and resulted in shallow colors.[42] As shown in Figure 4a, the RSA values of the lignin samples increased with the lignin concentration increase. EHL-ACLB showed higher RSA than EHL-LB and EHL within all lignin concentrations investigated. The IC_{50} values of different lignin samples are shown in Figure 4b; the order of IC_{50} values among different lignin samples was EHL-ACLB (0.49 mg/mL) < EHL-LB (0.54 mg/mL) < EHL (0.73 mg/mL), demonstrating that scavenging the same amount of DPPH radicals consumes less dosage of ACLB than other lignin samples. The photographs revealed that the DPPH methanol solution with EHL-ACLB addition exhibited the lightest color among all solutions examined, indicating that EHL-ACLB, possessing the highest phenolic groups, displayed the most potent radical scavenging capability.

3.3. Sunscreen Performance of MSH Treated Lignin. The absorption of organic molecules in UVB-UVA is mainly generated by $\pi \rightarrow \pi^*$ and $n \rightarrow \pi^*$.[43] Lignin is effective in absorbing UV radiation due to the presence of functional groups such as phenols, ketones, quinones, and other chromophores. The samples of EHL, EHL-LB, and EHL-ACLB were directly blended with the pure creams at concentrations of 2 wt %, and UV transmittances of the blended creams were measured. The pure cream without lignin exhibited a transmittance of approximately 100%, which means the pure cream does not contain sunscreen actives and barely

https://doi.org/10.1021/acsomega.4c08618
ACS Omega 2025, 10, 6745−6752

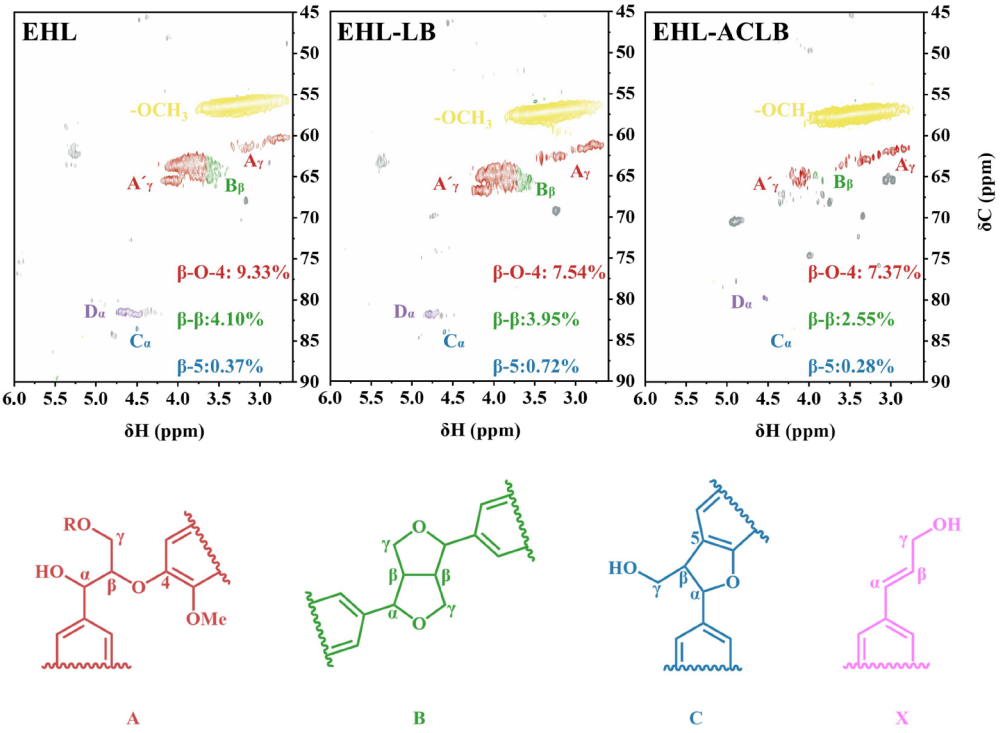

Figure 3. Aliphatic regions of the 2D HSQC spectra of EHL, EHL-LB, and EHL-ACLB in DMSO-d_6.

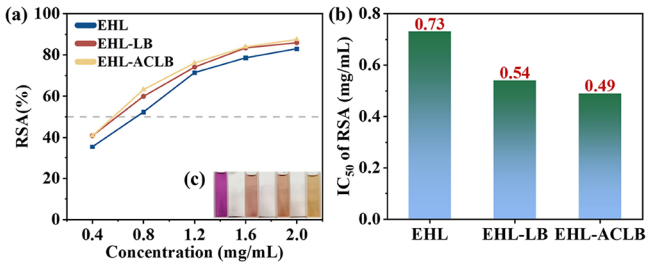

Figure 4. (a) RSA performance of EHL, EHL-LB, and EHL-ACLB. (b) IC_{50} values of EHL, EHL-LB, and EHL-ACLB. (c) Color comparison of DPPH, DPPH+EHL, DPPH+EHL-LB, and DPPH +EHL-ACLB.

exhibits sun protection ability. With the addition of lignin, the UV transmittance efficiently decreased (Figure 5a). Interestingly, it was found that after being treated with unacidified MSH, the UV absorption of lignin decreased and showed a limited SPF value of 1.90 (Figure 5b). The MSH treatment had possibly broken the $\pi-\pi$ stacking in the lignin structure[44]

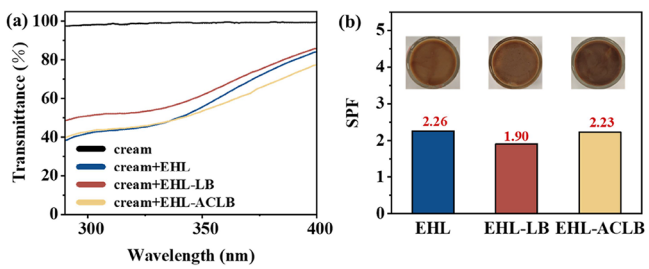

Figure 5. (a) UV transmittance with the addition of 2 wt % of EHL, EHL-LB, and EHL-ACLB to pure creams. (b) SPF value detected with the addition of 2 wt % EHL, EHL-LB, and EHL-ACLB to pure creams.

and resulted in a decrease in UV absorption caused by benzene ring stacking due to the existence of massive Br^-.[43] The acidified MSH treated EHL-ACLB resulted in a higher UV absorption ability and higher SPF value compared with EHL because a more serious structural condensation and aggregation occurred during MSH treatment assisted by HCl, which promoted UV absorption ability. Besides, EHL-LB showed a lighter color compared with EHL and EHL-ACLB, which was consistent with the lighter benzene ring stacking property of EHL. Therefore, modification of EHL with HCl acidified MSH can improve lignin antioxidation performance with a negligible effect on UV absorption ability.

3.4. Synthesis and Sunscreen Performance of LCSs.

The morphologies of lignin samples dispersed in the cream are shown in Figure S2 in the Supporting Information. The samples presented similar fragment states in the cream. The pure cream is a homogeneous water-in-oil (W/O) emulsion with hydrophilic functional groups distributed on the particle surfaces. When the lignin sample was added to the cream, the emulsion broke with lignin samples randomly dispersed in an irregular shape, suggesting poor compatibility with the cream, which might have negative effects on UV absorption. To address this issue, the modified lignin samples were transformed into hydrophilic LCSs to further improve their compatibility with the cream in order to improve UV absorption ability.

LCSs were transformed from EHL, EHL-LB, and EHL-ACLB via an antisolvent self-assembly method. Briefly, after a sufficient dissolution of a specific amount of lignin in the biphasic solvents consisting of acetone and water, deionized water was added to the mixture. Then, the dissolved lignin was transferred into LCSs under the influence of intermolecular forces and precipitated. SEM images of EHL-LCSs, LB-LCSs, and ACLB-LCSs are shown in Figure S3. The prepared EHL-LCSs, LB-LCSs, and ACLB-LCSs were blended with the pure

https://doi.org/10.1021/acsomega.4c08618
ACS Omega 2025, 10, 6745−6752

creams at concentrations of 2 wt % for sunscreen, and the UV transmittances of the blended creams were measured. As depicted in Figure S4, when mixed with the pure cream, LB-LCSs exhibited a W/O structure similar to that of the pure cream. In contrast, EHL-LCSs and ACLB-LCSs still displayed noticeable fragments, indicating that LB-LCSs have better compatibility with creams compared to EHL-LCSs and ACLB-LCSs. The UV transmittance spectra of the pure cream and the LCSs-doped sunscreens were detected and are presented in Figure 6a. The addition of LCSs significantly reduced the transmittance of the pure cream across the range of 290−400 nm. In particular, the UV transmittance of the cream blended with LB-LCSs was notably lower. Figure 6b shows that incorporating LB-LCSs into pure creams resulted in the highest SPF value of 4.66, which was twice as high as the direct addition of EHL and 1.4 times higher than that of EHL-LCSs. An unconventional finding revealed that despite having the highest phenolic hydroxyl groups, the LCSs prepared from EHL-ACLB self-assembly still exhibited inefficient UV absorption performance compared to LB-LCSs. This calls for a deeper understanding of the underlying factors contributing to this discrepancy.

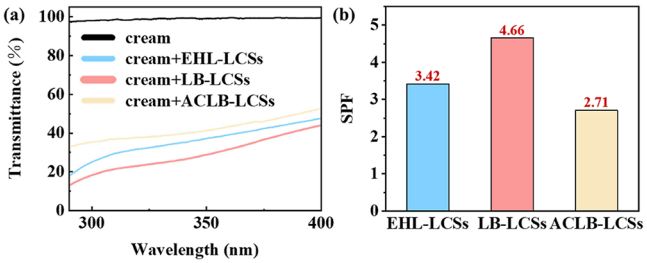

Figure 6. (a) UV transmittance after adding 2 wt % of LCSs, LB-LCSs, and ACLB-LCSs to pure creams. (b) SPF after addition of 2 wt % LCSs, LB-LCSs, and ACLB-LCSs to pure creams.

In addition to molecular structure, the lignin aggregation state can critically affect some macroscopic performance, such as solubility in water and interfacial compatibility with sunscreen. Based on the SEM results, the limited UV absorption ability of ACLB-LCSs dispersed creams can be due to the limited compatibility of ACLB-LCSs with creams. The aggregation state of lignin samples was evaluated by the quantification of lignin intermolecular forces in water with AFM spectra. As shown in Figure 7, the intermolecular adhesive force values for EHL, EHL-LB, and EHL-ACLB are −1.46 ± 0.16, −0.46 ± 0.26, and −0.61 ± 0.16 mN/m, respectively (a negative value means that the forces are attractive). The higher adhesive force value refers to higher lignin structural aggregation, which decreases lignin hydrophilicity and compatibility with the W/O emulsion of pure creams.

In order to investigate the impact of the average particle size of LCSs on their UV transmittance, lignin solutions with concentrations of 2, 4, and 6 g/L were prepared by using EHL as a raw material. Subsequently, LCSs-2, LCSs-4, and LCSs-6 were synthesized through antisolvent self-assembly. The average particle size of LCSs increased proportionally with the concentration of the lignin solution (Figure 8). Notably, LCSs-2 exhibited the smallest average particle size at 568 nm and demonstrated the lowest UV transmittance. This observation may be attributed to the high specific surface area of smaller particles, leading to homogeneous blending with creams.[45]

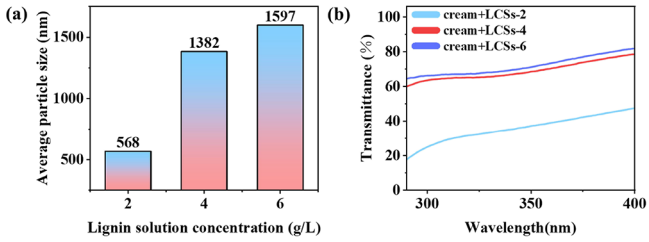

Figure 8. (a) Average particle size of LCSs-2, LCSs-4, and LCSs-6. (b) UV transmittance after adding 2 wt % of LCSs-2, LCSs-4, and LCSs-6 to pure creams.

4. CONCLUSIONS

A high-quality lignin with abundant phenolic hydroxyl groups and strong hydrophilicity was derived from industrial lignin in MSH, exhibiting exceptional antioxidation and UV absorption capabilities. The unacidified MSH facilitated the cleavage of ether bonds to generate phenolic hydroxyl groups without inducing structural condensation. Upon transformation into LCSs, the lignin's hydrophilicity was further enhanced, thereby improving its compatibility and dispersibility in creams. While the addition of concentrated HCl acid can increase the content of phenolic hydroxyl groups, it may simultaneously elevate intermolecular adhesive forces, leading to a reduction in lignin's hydrophilicity and UV absorption capacity. This study presents a straightforward approach for preparing highly active lignin from industrial sources with potential applications in antioxidation and UV protection.

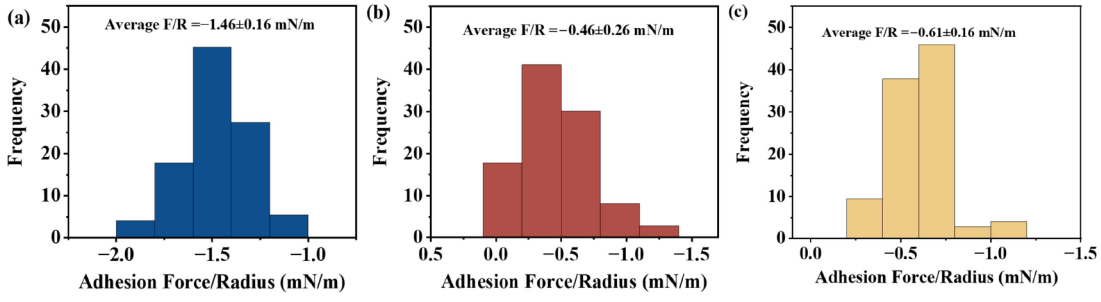

Figure 7. Histogram of the distribution of intermolecular forces in EHL (a), EHL-LB (b), and EHL-ACLB (c).

https://doi.org/10.1021/acsomega.4c08618
ACS Omega 2025, 10, 6745−6752

■ ASSOCIATED CONTENT

Supporting Information

The Supporting Information is available free of charge at https://pubs.acs.org/doi/10.1021/acsomega.4c08618.

^{1}H NMR spectrum of EHL, EHL-LB, and EHL-ACLB; microscopy of cream + EHL, cream + EHL-LB, and cream + EHL-ACLB; SEM of cream + EHL-LCSs, cream + LB-LCSs, and cream + ACLB-LCSs; and microscopy of cream + EHL-LCSs, cream + LB-LCSs, and cream + ACLB-LCSs (Figures S1−S4) (PDF)

■ AUTHOR INFORMATION

Corresponding Authors

Qiyu Liu − *Guangdong Provincial Key Laboratory of Plant Resources Biorefinery, School of Chemical Engineering and Light Industry, Guangdong University of Technology, Guangzhou 510006, China; Guangdong Provincial Laboratory of Chemistry and Fine Chemical Engineering Jieyang Center, Jieyang 515200, China; Guangdong Basic Research Center of Excellence for Ecological Security and Green Development in Guangdong-Hong Kong-Marco Greater Bay Area (GBA), Guangdong University of Technology, Guangzhou 510006, China;* orcid.org/0000-0002-6860-5028; Email: liuqiyu@gdut.edu.cn

Xueqing Qiu − *Guangdong Provincial Key Laboratory of Plant Resources Biorefinery, School of Chemical Engineering and Light Industry, Guangdong University of Technology, Guangzhou 510006, China; Guangdong Provincial Laboratory of Chemistry and Fine Chemical Engineering Jieyang Center, Jieyang 515200, China; Guangdong Basic Research Center of Excellence for Ecological Security and Green Development in Guangdong-Hong Kong-Marco Greater Bay Area (GBA), Guangdong University of Technology, Guangzhou 510006, China;* orcid.org/0000-0001-8765-7061; Email: cexqqiu@scut.edu.cn

Authors

Lili He − *Guangdong Provincial Key Laboratory of Plant Resources Biorefinery, School of Chemical Engineering and Light Industry, Guangdong University of Technology, Guangzhou 510006, China; Guangdong Provincial Laboratory of Chemistry and Fine Chemical Engineering Jieyang Center, Jieyang 515200, China; Guangdong Basic Research Center of Excellence for Ecological Security and Green Development in Guangdong-Hong Kong-Marco Greater Bay Area (GBA), Guangdong University of Technology, Guangzhou 510006, China*

Haiping Guo − *Guangdong Provincial Key Laboratory of Plant Resources Biorefinery, School of Chemical Engineering and Light Industry, Guangdong University of Technology, Guangzhou 510006, China; Guangdong Provincial Laboratory of Chemistry and Fine Chemical Engineering Jieyang Center, Jieyang 515200, China; Guangdong Basic Research Center of Excellence for Ecological Security and Green Development in Guangdong-Hong Kong-Marco Greater Bay Area (GBA), Guangdong University of Technology, Guangzhou 510006, China*

Jiayue Lu − *Guangdong Provincial Key Laboratory of Plant Resources Biorefinery, School of Chemical Engineering and Light Industry, Guangdong University of Technology, Guangzhou 510006, China; Guangdong Provincial Laboratory of Chemistry and Fine Chemical Engineering Jieyang Center, Jieyang 515200, China; Guangdong Basic Research Center of Excellence for Ecological Security and Green Development in Guangdong-Hong Kong-Marco Greater Bay Area (GBA), Guangdong University of Technology, Guangzhou 510006, China*

Complete contact information is available at: https://pubs.acs.org/10.1021/acsomega.4c08618

Notes

The authors declare no competing financial interest.

■ ACKNOWLEDGMENTS

This study was supported by the National Natural Science Foundation of China (22378077, U23A6005), Guangzhou Basic and Applied Basic Research Foundation (2024A04J4434), Guangdong Basic and Applied Basic Research Foundation (2023A1515010064), and Young Elite Scientists Sponsorship Program by CAST (2023QNRC001). The authors acknowledge the Analysis and Test Center, Guangdong University of Technology for the structural analysis (NMR and SEM) of our samples.

■ REFERENCES

(1) Gonzaga, E. R. Role of UV light in photodamage, skin aging, and skin cancer: importance of photoprotection. *Am. J. Clin Dermatol.* **2009**, *10*, 19−24.

(2) Lim, H. W.; Kohli, I.; Ruvolo, E.; Kolbe, L.; Hamzavi, I. H. Impact of visible light on skin health: The role of antioxidants and free radical quenchers in skin protection. *J. Am. Acad. Dermatol.* **2022**, *8*, 27−37.

(3) Michalak, M. Plant-derived antioxidants: Significance in skin health and the ageing process. *Int. J. Mol. Sci.* **2022**, *23*, 585.

(4) Zhang, Y.; Naebe, M. Lignin: A review on structure, properties, and applications as a light-colored UV absorber. *Acs Sustain Chem. Eng.* **2021**, *9*, 1427−1442.

(5) Wu, Y.; Qian, Y.; Lou, H.; Yang, D.; Qiu, X. Enhancing the broad-spectrum adsorption of lignin through methoxyl activation, grafting modification, and reverse self-assembly. *Acs Sustain Chem. Eng.* **2019**, *7*, 15966−15973.

(6) Pan, X.; Kadla, J. F.; Ehara, K.; Gilkes, N.; Saddler, J. N. Organosolv ethanol lignin from hybrid poplar as a radical scavenger: relationship between lignin structure, extraction conditions, and antioxidant activity. *J. Agric. Food Chem.* **2006**, *54*, 5806−5813.

(7) Spiridon, I. Extraction of lignin and therapeutic applications of lignin-derived compounds. *A review. Environ. Chem. Lett.* **2020**, *18*, 771−785.

(8) Mondal, S.; Jatrana, A.; Maan, S.; Sharma, P. Lignin modification and valorization in medicine, cosmetics, environmental remediation and agriculture: a review. *Environ. Chem. Lett.* **2023**, *21*, 2171−2197.

(9) Tran, M. H.; Phan, D. P.; Lee, E. Y. Review on lignin modifications toward natural UV protection ingredient for lignin-based sunscreens. *Green Chem.* **2021**, *23*, 4633−4646.

(10) Wu, X.; Zhou, M.; Ouyang, X.; Qiu, X.; Qian, Y. Whiten Lignin-Based Sunscreen via Fractionation and Ultrasonic Cavitation. *ACS Sustain. Chem. Eng.* **2024**, *12*, 6539−6546.

(11) Fan, Y. F.; Ji, H. R.; Ji, X. X.; Tian, Z. J.; Chen, J. C. Lignocellulosic biomass pretreatment with a lignin stabilization strategy and valorization toward multipurpose fractionation. *Int. J. Biol. Macromol.* **2024**, *259*, No. 129186.

(12) Sadeghifar, H.; Ragauskas, A. Lignin as a UV Light Blocker-A Review. *Polymers* **2020**, *12*, 1134.

(13) Piccinino, D.; Capecchi, E.; Tomaino, E.; Gabellone, S.; Gigli, V.; Avitabile, D.; Saladino, R. Nano-structured lignin as green antioxidant and UV shielding ingredient for sunscreen applications. *Antioxidants.* **2021**, *10*, 274.

(14) Qian, Y.; Qiu, X.; Zhu, S. Lignin: a nature-inspired sun blocker for broad-spectrum sunscreens. *Green Chem.* **2015**, *17*, 320−324.
(15) You, S.; Xie, Y.; Zhuang, X.; Chen, H.; Qin, Y.; Cao, J.; Lan, T. Effect of high antioxidant activity on bacteriostasis of lignin from sugarcane bagasse. *Biochem. Eng. J.* **2022**, *180*, No. 108335.
(16) Lourençon, T. V.; de Lima, G. G.; Ribeiro, C. S.; Hansel, F. A.; Maciel, G. M.; da Silva, K.; Winnischofer, S. M.; de Muniz, G. I.; Magalhães, W. L. B. M. Antibacterial and antitumoural activities of kraft lignin from hardwood fractionated by acid precipitation. *Int. J. Biol. Macromol.* **2021**, *166*, 1535−1542.
(17) do Nascimento Santos, D. K. D.; da Silva Barros, B. R.; de Souza Aguiar, L. M.; da Cruz Filho, I. J.; de Lorena, V. M. B.; de Melo, C. M. L.; Napoleão, T. H. Immunostimulatory and antioxidant activities of a lignin isolated from Conocarpus erectus leaves. *Int. J. Biol. Macromol.* **2020**, *150*, 169−177.
(18) Guo, Z.; Li, D.; You, T.; Zhang, X.; Xu, F.; Zhang, X.; Yang, Y. New lignin streams derived from heteropoly acids enhanced neutral deep eutectic solvent fractionation: toward structural elucidation and antioxidant performance. *Acs Sustain Chem. Eng.* **2020**, *8*, 12110−12119.
(19) Zhong, L.; Wang, C.; Xu, M.; Ji, X.; Yang, G.; Chen, J.; Janaswamy, S.; Lyu, G. Alkali-catalyzed organosolv pretreatment of lignocellulose enhances enzymatic hydrolysis and results in highly antioxidative lignin. *Energy & Fuels.* **2021**, *35*, 5039−5048.
(20) Gong, Z.; Shuai, L. Lignin condensation, an unsolved mystery. *Trends Chem.* **2023**, *5*, 163−166.
(21) Kazzaz, A. E.; Fatehi, P. Fabrication of amphoteric lignin and its hydrophilicity/oleophilicity at oil/water interface. *J. Colloid Interface Sci.* **2020**, *561*, 231−243.
(22) Alwadani, N.; Ghavidel, N.; Fatehi, P. Surface and interface characteristics of hydrophobic lignin derivatives in solvents and films. *Colloid Surface A* **2021**, *609*, No. 125656.
(23) Zhang, A.; Wu, X.; Ouyang, X.; Lou, H.; Yang, D.; Qian, Y.; Qiu, X. Preparation of light-colored lignosulfonate sunscreen microcapsules with strengthened UV-blocking and adhesion performance. *Acs Sustain Chem. Eng.* **2022**, *10*, 9381−9388.
(24) Wang, Y.; Du, B.; Zheng, Q.; Chen, X. A demethylated lignin improved PVA-based supramolecular plastic with tough, degradable, and water-resistant performances. *Int. J. Biol. Macromol.* **2024**, *276*, No. 133610.
(25) Venkatesagowda, B.; Dekker, R. F. Microbial demethylation of lignin: Evidence of enzymes participating in the removal of methyl/methoxyl groups. *Enzyme Microb Technol.* **2021**, *147*, No. 109780.
(26) Liu, P. C.; Guo, Y. L.; Guo, G.; Dai, L.; Hu, G.; Xie, H. B. Lignin-grafting alternative copolymer of 3,4-dihydrocoumarin and epoxides as an active and flexible ingredient in sunscreen. *Green Chem.* **2023**, *25*, 4469−4481.
(27) Tang, Q. Q.; Zhou, M. S.; Yang, D. J. Preparation of uniform lignosulfonate-based colloidal spheres for UV-absorbing thermoplastics. *Int. J. Biol. Macromol.* **2022**, *219*, 663−671.
(28) Izaguirre, N.; Fernández-Rodríguez, J.; Robles, E.; Labidi, J. Sonochemical oxidation of technical lignin to obtain nanoparticles with enhanced functionality. *Green Chem.* **2023**, *25*, 8808−8819.
(29) Yu, H. A.; Wang, B. J.; Wang, Y. M.; Xu, E. H.; Wang, R.; Wu, S. Y.; Wu, W.; Ji, B. L.; Feng, X. L.; Xu, H.; Zhong, Y.; Mao, Z. P. Lignin Nanoparticles with High Phenolic Content as Efficient Antioxidant and Sun-Blocker for Food and Cosmetics. *ACS Sustain. Chem. Eng.* **2023**, *11*, 4082−4092.
(30) Yang, X.; Li, Z.; Li, L.; Li, N.; Jing, F.; Hu, L.; Shang, Q.; Zhang, X.; Zhou, Y.; Pan, X. Depolymerization and demethylation of kraft lignin in molten salt hydrate and applications as an antioxidant and metal ion scavenger. *J. Agric. Food Chem.* **2021**, *69*, 13568−13577.
(31) Yang, X.; Li, N.; Lin, X.; Pan, X.; Zhou, Y. Selective cleavage of the aryl ether bonds in lignin for depolymerization by acidic lithium bromide molten salt hydrate under mild conditions. *J. Agric. Food Chem.* **2016**, *64*, 8379−8387.
(32) Liu, Q.; Zhang, H. N.; Ren, H.; Zhai, H. M. Structural analysis of light-colored separated lignin (lignocresol) and its antioxidant properties. *Int. J. Biol. Macromol.* **2022**, *197*, 169−178.
(33) Lee, S. C.; Yoo, E.; Lee, S. H.; Won, K. Preparation and Application of Light-Colored Lignin Nanoparticles for Broad-Spectrum Sunscreens. *Polymers.* **2020**, *12*, 699.
(34) Wang, J.; Chen, W.; Yang, D.; Fang, Z.; Liu, W.; Xiang, T.; Qiu, X. Monodispersed Lignin Colloidal Spheres with Tailorable Sizes for Bio-Photonic Materials. *Small* **2022**, *18*, No. e2203561.
(35) Wang, J.; Qian, Y.; Li, L.; Qiu, X. Atomic force microscopy and molecular dynamics simulations for study of lignin solution self-assembly mechanisms in organic−aqueous solvent mixtures. *ChemSusChem* **2020**, *13*, 4420−4427.
(36) Horikawa, Y.; Hirano, S.; Mihashi, A.; Kobayashi, Y.; Zhai, S. C.; Sugiyama, J. Prediction of Lignin Contents from Infrared Spectroscopy: Chemical Digestion and Lignin/Biomass Ratios of Cryptomeria japonica. *Appl. Biochem. Biotechnol.* **2019**, *188*, 1066−1076.
(37) Liu, C.; Hu, J.; Zhang, H.; Xiao, R. Thermal conversion of lignin to phenols: Relevance between chemical structure and pyrolysis behaviors. *Fuel.* **2016**, *182*, 864−870.
(38) Meng, X.; Crestini, C.; Ben, H.; Hao, N.; Pu, Y.; Ragauskas, A. J.; Argyropoulos, D. S. Determination of hydroxyl groups in biorefinery resources via quantitative ^{31}P NMR spectroscopy. *Nat. Protoc.* **2019**, *14*, 2627−2647.
(39) Li, Z.; Sutandar, E.; Goihl, T.; Zhang, X.; Pan, X. J. Cleavage of ethers and demethylation of lignin in acidic concentrated lithium bromide (ACLB) solution. *Green Chem.* **2020**, *22*, 7989−8001.
(40) Dizhbite, T.; Telysheva, G.; Jurkjane, V.; Viesturs, U. Characterization of the radical scavenging activity of lignins−−natural antioxidants. *Bioresour. Technol.* **2004**, *95*, 309−317.
(41) Gulcin, İ. Antioxidants and antioxidant methods: An updated overview. *Arch. Toxicol.* **2020**, *94*, 651−715.
(42) Zhao, X.; Wan, H.-F.; Sun, S.-F.; Gao, C.; Zhang, S.; Sun, R.-C. Industrial lignin activation with enhanced antioxidant capability in mild halogen-free protic ionic liquids. *Ind. Crop Prod.* **2024**, *219*, No. 119020.
(43) Li, Y. R.; Zhao, S. Y.; Hu, D. B.; Ragauskas, A. J.; Cao, D. Y.; Liu, W. Q.; Si, C. L.; Xu, T.; Zhao, P. T.; Song, X. P.; Li, K. Role Evaluation of Active Groups in Lignin on UV-Shielding Performance. *ACS Sustain. Chem. Eng.* **2022**, *10*, 11856−11866.
(44) Han, X.; Wei, Q.; Su, Y.; Che, G.; Zhou, J.; Li, Y. Molecular modification of lignin-based carbon materials: influence of supramolecular bonds on the properties. *ACS Appl. Mater.* **2023**, *15*, 1969−1983.
(45) Ariyanta, H. A.; Santoso, E. B.; Suryanegara, L.; Arung, E. T.; Kusuma, I. W.; Taib, M.; Hussin, M. H.; Yanuar, Y.; Batubara, I.; Fatriasari, W. Recent Progress on the Development of lignin as future ingredient biobased cosmetics. *Sustainable Chem. Pharm.* **2023**, *32*, No. 100966.

https://doi.org/10.1021/acsomega.4c08618
ACS Omega 2025, 10, 6745−6752